Supplementary materials for: Real-time fMRI functional connectivity neurofeedback reducing repetitive negative thinking in depression: a double-blind, randomized, sham-controlled proof-of-concept trial

Aki Tsuchiyagaito[a,b,c,*,#], Masaya Misaki[a,*], Namik Kirlic[a], Xiaoqian Yu[a], Stella M. Sánchez[a], Gabe Cochran[a], Jennifer L. Stewart[a,b], Ryan Smith[a,b], Kate D. Fitzgerald[d], Michael L. Rohan[a], Martin P. Paulus[a], Salvador M. Guinjoan[a,e]

[a] Laureate Institute for Brain Research, Tulsa, OK, USA

[b] Oxley College of Health Sciences, The University of Tulsa, Tulsa, OK, USA

[c] Research Center for Child Mental Development, Chiba University, Chiba, Japan

[d] Department of Psychiatry, Columbia University, New York, NY, USA

[e] Department of Psychiatry, Oklahoma University Health Sciences Center at Tulsa, Tulsa, OK, USA

[*] These authors contributed equally to this work.

Short Title: Connectivity neurofeedback reducing RNT

[#] Corresponding Author:

Aki Tsuchiyagaito

Laureate Institute for Brain Research

6655 South Yale Ave. Tulsa, OK 74136, USA

Tel: 918-502-5112

E-mail: atsuchiyagaito@laureateinstitute.org

Table of Contents

1 Supplementary Introduction

1.1 Region-of-interest (ROI)-based and connectivity-based rtfMRI-nf

The majority of rt-fMRI-nf studies so far have used region-of-interest (ROI) based techniques where feedback from the activity in a single ROI was the training target. These investigations effectively showed that self-regulating the target brain activity was possible [1], and concomitant symptom relief could be observed [2,3]. Beyond the ROI approach, in recent years, a shift in the emphasis on connectivity-based techniques has developed. According to early findings of connectivity-based rtfMRI-nf studies, it is possible to cause a self-regulation in functional connectivity accompanied by symptom changes [4-6]. Connectivity-based rtfMRI-nf holds significant potential, particularly for developing transdiagnostic treatments addressing certain neural circuits associated with specific mental diseases (e.g., dysfunction of a particular network such as the default mode network: DMN, coupled with deficits in a self-referential processing represented by RNT) [7-13].

1.2 The rationale for modulating the PCC-rTPJ connectivity to reduce RNT

Our prior work searched for the functional connectivity associated with RNT using the resting-state fMRI data in individuals with mood and anxiety disorders [14]. Our data-driven approach identified that connectivity between the precuneus/posterior cingulate cortex (PCC) and right temporoparietal junction (rTPJ) was positively correlated with levels of RNT [14]. Both the PCC and the rTPJ appear to play an important role in self-referential processing as part of the default mode network (DMN) [15,16]. The PCC serves as a hub of the DMN, engaging in a self-related mental activity [17-19], while the rTPJ is related to an emotional processing, empathy, and the theory of mind (ToM) [20-22]. This RNT-related PCC-rTPJ hyperconnectivity pattern suggests that overly self-focused self-referential processing might be an underlying feature of RNT. In our previous study, we successfully used rtfMRI-nf to reduce PCC-rTPJ connectivity in healthy participants [23].

1.3 The rationale for the control condition

Three recent RCTs comparing active vs. control rtfMRI-nf in MDD showed mixed findings [24-26]. One study found that training to increase activation in the amygdala was effective in reducing depression as compared to activation within the intraparietal sulcus [26]. In contrast, two other studies did not find an effect of active training, one case using rtfMRI-nf based on a measure of blame-related connectivity as an adjunct compared to no rtfMRI-nf, and in the other case using rtfMRI based on activation within emotional brain regions as compared to activation within visual cortex [24,25]. Importantly, in those two studies, the sense of achievement (e.g., self-efficacy experienced by participants when they believe they are controlling their brain activity) was associated with symptom reduction regardless of learned control of activation or connectivity within the brain [24,25]. With rtfMRI-nf, individuals learn to regulate their neural activity by receiving reinforcing feedback regarding desired brain changes. Sensory feedback informs participants about their corresponding reward, and there is a chance

that reward experiences during rtfMRI-nf have a therapeutic effect [25,27]. Thus, this RCT utilized active sham-controlled feedback where participants received artificially generated feedback with similar probabilistic properties to the real feedback to control reward experiences.

2 Supplementary Methods

2.1 Random group assignment and blinding

One of the investigators (MM) was responsible for participants' randomization. This investigator was not involved in any data collection, nor in interactions with the study participants. Recruitment, informed consent, and rtfMRI-nf were conducted by another researcher (AT) unaware of and not involved with the randomization. Interview-based assessments were conducted by raters who were also not aware of randomization procedures. In order to maintain the participants', the coordinator's, and the raters' blind status, a group assignment was conducted as follows: when a subject was ready to be in the MRI to perform rtfMRI-nf training, the investigator responsible for verum or sham assignment, remotely logged in to the rtfMRI-nf computer system, and set up the active or sham procedure in the computer system. The study participant and the researcher were able to see a series of binary feedback (blue bars: +1 or blank bars: 0, see suppl. Methods 2.7) either from the target PCC-rTPJ connectivity (active) or artificially simulated signals (sham). However, they were not notified which group the participant was assigned to. In this way, participants, the researcher who interacted with them, and raters, were all fully blind to the group assignment.

2.2 Sample size calculation

The sample size was estimated with the R package SIMR (https://cran.r-project.org/web/packages/simr/index.html), which allows power calculations of the linear mixed effect model (LME) and is based on Monte Carlo simulations [28]. Sample size calculations for the primary outcome were based on our previous data where 28 healthy participants (n=14 per active and sham group, respectively) [23]. The sample size estimation was based on changes in our primary outcome, PCC-rTPJ connectivity. The model included the interaction of time (NF1, NF2, NF3, and View2) and group (active and sham). The model also had a subject as a random effect to account for repeated measurements. We used the power curve function to explore trade-offs between power and sample size.

Our previous pilot data with healthy participants [23] showed a large effect size for the interaction term ($F[3,78] = 6.94$, $p < 0.001$, $\omega^2 = 0.15$). Since this observed large effect size relied on healthy participants' data, and we were not certain whether subjects with MDD would be able to achieve this level of effect size, we conservatively estimated the effect size as medium ($F[3,78] = 2.75$, $p < 0.05$, $\omega^2 = 0.06$) (the effect size interpretation; $0.01 \leq \omega^2 < 0.06$: small; $0.06 \leq \omega^2 < 0.14$: Medium; and $0.14 \leq \omega^2$[29]) for our simulation. Utilizing SIMR package, we simulated the power curve to detect the medium effect size ($\omega^2 = 0.06$) for the time-by-group interaction term. The analysis showed that to detect a significant difference in the interaction term with an effect size (ω^2) of 0.06 between the active and sham groups, we need at least 19 participants

(to have 80% power and a significant threshold of $\alpha = 0.05$, two-sided) in each group (Fig. S1). Considering a 10% attrition rate, we planned to recruit 42 subjects overall.

2.3 Neuroimaging data acquisition and preprocessing

Imaging was conducted on a 3Tesla MR750 Discovery (GE Healthcare, Milwaukee, WI) with an 8-channel receive-only head array coil. The fMRI acquisition was a gradient Echo Planar Imaging sequence with TE/TR=25ms/2s; matrix 96 on a 240mm FOV, 40 slices at 2.9mm; SENSE = 2. BOLD fMRI data were acquired using a T2*-weighted gradient echo-planar sequence with sensitivity encoding (GE-EPI SENSE) with the following parameters: TR/TE=2000/25 ms, acquisition matrix=96 × 96, FOV/slice=240/2.9 mm, flip angle=90°, voxel size 2.5×2.5×2.9 mm; 40 axial slices, SENSE acceleration R=2. For anatomical reference, T1-weighted (T1w) MRI images were acquired with a magnetization-prepared rapid gradient-echo (MPRAGE) sequence with parameters of FOV= 240×192 mm, matrix=256×256, 124 axial slices, slice thickness=1.2 mm, 0.94×0.94×1.2 mm^3 voxel volume, TR/TE=5/2 ms, SENSE acceleration R=2, flip angle=8°, delay/inversion time TD/TI=1400/725 ms, sampling bandwidth=31.2 kHz, scan time = 4 min 59 s.

2.4 Real-time fMRI processing

An in-house program written in Python was used for real-time fMRI data transferring and processing with comprehensive noise reduction and motion correction [30,31]. The real-time fMRI processing included slice-timing correction, motion correction, spatial smoothing with 6mm-FWHM Gaussian kernel within the brain mask, scaling to a percent change relative to the average for the first 28 TRs (in the initial rest period), and regressing out noise components [30-32]. The noise regressors were 12 motion parameters (three shifts, three rotations, and their temporal derivatives), eight RETROICOR [33] regressors (four cardiac and four respiration), global signal, white matter mean signal, ventricle mean signal, and Legendre polynomial models of slow signal fluctuation. This comprehensive noise reduction was performed in real-time (less than 400 ms) [30-32].

The masks for the white matter and ventricles regions and the ROIs of precuneus and rTPJ were defined in the MNI template brain. The ROIs were defined as spheres of a 6 mm radius at the precuneus locus (MNI: -6, -58, 48) and the rTPJ (MNI: 51, -49, 23) in accordance with our previous research [14]. These masks and ROIs in the MNI space were warped to the individual subject's brain for real-time signal calculation (Fig. S2). At first, a subject's anatomical image was aligned to a functional image of the first functional run (resting-state scan). Then, the MNI template brain was warped to the aligned anatomical image using the Advanced Normalization Tools (ANTs, [34]; http://stnava.github.io/ANTs/). Finally, the warped masks and ROIs were resampled in functional image resolution to make masks and ROIs in the functional image space for real-time calculation. The processing of the masks and ROIs were done before the neurofeedback runs. The functional image used as a reference for the alignment and resampling was also used as a reference for the real-time motion correction.

2.5 rtfMRI-nf training paradigm

The rtfMRI-nf training paradigm was the same as in our previous study [23] and illustrated in Fig. S3. Briefly, each of the five 8-mins experimental runs (View1, NF1, NF2, NF3, and View2) started with a 90-sec initial resting block, followed by three 130-sec trial blocks, each composed of a 100-sec regulation block with four consecutive presentations of negative trait words (25-sec each; see list of stimulus words in Table S2), and a 30-sec rest. During the regulation block, a subject attempted to regulate RNT using reappraisal (i.e., emotion regulation strategy to reinterpret their negative self-perspectives) while viewing negative words describing their negative personality traits (detailed description of emotion regulation instructions can be found in suppl. Methods 2.6). Neurofeedback was presented in the middle three experimental runs (NF1, NF2, and NF3), but not in the first and last two experimental runs (View1 and View2). The View1 and View2 non-neurofeedback runs were used to assess changes in PCC-rTPJ connectivity in the absence of neurofeedback signals, and PCC-rTPJ connectivity during View1 was used as baseline connectivity for each participant.

2.6 Explicit emotion regulation strategies to regulate RNT-related connectivity

For the resting block, participants were instructed to look at the fixation cross displayed at the center of the presentation screen and not to think of anything in particular. For the regulation block, participants were instructed to apply an emotion regulation strategy, such as cognitive reappraisal [35,36], while viewing negative words describing their negative personality traits (see details in Table S2). Examples of cognitive reappraisal were provided prior to the intervention: "Everyone has these negative traits;" "Sometimes, I behave like that, but not always;" and "Thinking about the good side of the negative trait." The participants in both groups were instructed that the presence of blue sidebars indicates the subject's brain status is in the desired state (subject is successful in controlling the RNT-related brain circuit), and were instructed to try and adjust their emotion regulation strategies based on the provided feedback throughout the experimental runs. Also, they were informed that there would be a 7-sec hemodynamic delay between brain changes and feedback signals and that their goal was to keep the sidebars blue as long as possible.

Since participants had not experienced rtfMRI-nf at View1 yet, they were simply asked to use their usual emotional regulation strategies to regulate RNT. In the last view condition (View2: Transfer), they were instructed to use the emotion regulation strategy that worked best throughout the three neurofeedback runs. The View1 and View2 non-neurofeedback runs were used to assess changes in the target connectivity between the PCC and rTPJ in the absence of neurofeedback signals, and PCC-rTPJ connectivity during View1 was used as baseline connectivity for each participant.

2.7 Neurofeedback signal calculation utilizing a two-point method and sham feedback

Our previous study [14] performed a simulation analysis to optimize an algorithm for online real-time connectivity feedback signals to reduce the connectivity between the two target ROIs (i.e., the PCC and rTPJ). We evaluated several approaches of online connectivity calculations, i.e., sliding-window correlation [37] and the two-point method [38]. The original introduction of the two-point method utilized a control ROI to cancel a signal change unspecific to the target connectivity [38]. Both versions of the two-point method, with and without the control ROI, were

evaluated in the simulation. The simulation was performed on an advanced rtfMRI data processing system implementing comprehensive online noise reduction processes [30-32], which is the same system used for the current rtfMRI-nf, with slice-timing correction, motion correction, spatial smoothing, signal scaling and GLM with regressors of high-pass filtering, six motion parameters, mean white matter signal, mean ventricle signal, and RETROICOR [33] for the estimation of online connectivity. The optimality of online feedback signals was evaluated with regard to three criteria, i.e., a correlation between online connectivity and offline connectivity, robustness to head motion, and timeliness of neurofeedback. The simulation results indicated a trade-off between the correlation with offline connectivity and the risk of motion contamination. The higher correlation between online connectivity and offline connectivity was observed with more time points (i.e., sliding-window correlations with ten time points); however, the more time points were included, the more the feedback signal was correlated with head motions. Dependence of long signal history is also not favored regarding the timeliness of the neurofeedback. Including the control ROI in the two-point method decreased the correlation between online connectivity and offline connectivity, which could be attributed to a reduced positive feedback frequency with restriction by the control ROI. Therefore, we decided to utilize the two-point method without the control ROI for this study because it was robust to motion, less dependent on signal history, and more time sensitive for training to decouple the target functional connectivity(see more details in [14]). The two-point method calculates a signal change direction in a consecutive two-time points window and compares the change directions of the two target ROIs as a proxy measure of online connectivity. The feedback signal is calculated as a binary value. When the BOLD signal from the PCC and the rTPJ moved in different directions (i.e., the change of BOLD signal from the PCC increased and that from the rTPJ decreased, or that from the PCC decreased and that from the rTPJ increased), participants saw blue bars displayed on both sides of the word stimulus as positive neurofeedback (coded as +1) (Figs. S3 and S4. A). When the changes of the BOLD signal from the PCC and the rTPJ moved in the same direction, participants saw blank sidebars, which indicated the absence of feedback (coded as 0). The neurofeedback presentation started 8 sec after the onset of the Regulation block to wait for the hemodynamic response delay and to sample two points for connectivity calculation.

The participants assigned to the sham group received the same feedback presentation as the active group did, except that the feedback signals were artificially generated and unrelated to the target connectivity. Prior to the enrollment of the first participants, we conducted a small pilot study with seven MDD-affected volunteers who underwent active rtfMRI-nf. Based on those preliminary data, we calculated conditional probabilities of positive feedback following the positive and no feedback events, $P(FB_{+1}|FB_0)$ and $P(FB_{+1}|FB_{+1})$. The sham feedback signal was made following these probabilities. The initial feedback in each block was determined by the unconditional probability, $P(FB_{+1})$. After the enrollment of the first participant of the current study, every time a participant in the active group was enrolled, these probabilities were updated and used for synthesized sham feedback.

2.8 A safeguard to avoid accidental correlation between synthesized sham and actual functional connectivity in the sham group

For the sham group, we calculated the correlation between the time courses of synthesized sham signals and the actual target connectivity in a real-time during the scan. If the absolute correlation surpassed the threshold (> 0.3), the feedback signal was made to reduce the absolute correlation regardless of the probability. The positive feedback probability for each sham participant was also monitored in real-time, and if it diverged from the defined one, $P(FB_{+1})$, the feedback signal was made to adjust it.

2.9 Primary neural outcome: changes in PCC-rTPJ connectivity

Analysis of Functional NeuroImages package (AFNI; http://afni.nimh.nih.gov/)[39] was employed for processing. The first three TRs were discarded from the analysis. The process included despike, RETROICOR [33] and respiration volume per time (RVT) correction [40], slice-timing and motion corrections, nonlinear warping to the MNI template brain with resampling to $2mm^3$ voxels using the ANTs (http://stnava.github.io/ANTs/), spatial smoothing with 6mm-FWHM Gaussian kernel, and scaling signal to percent change relative to the mean in each voxel. Any time point with large motion (> 0.30 mm frame-wise displacement (FD)) was censored within the regression [41]. Scans censored 25% or more were not used for subsequent analyses and were treated as missing values. For the generalized psychophysiological interaction (gPPI) analysis [42], the design matrix of the general linear model (GLM) analysis for PPI included regressors of the task block modeled with a box-car function convolved with hemodynamic response function (HRF), the three stimulus presentations ('word change,' 'change to the positive feedback,' 'change to no feedback') modeled with a delta function convolved with HRF, and the PPI regressors of the PCC ROI signal time series and the multiplication of the task-block regressor and the ROI-signal regressor as an interaction term. The design matrix also included noise regressors of three principal components of the ventricle signal, local white matter average signal (ANATICOR) [43], 12 motion parameters (three shift and three rotation parameters with their temporal derivatives), and low-frequency fluctuation (third-order Legendre polynomial model). The ROI signal time series was extracted from the residual signal of the GLM analysis with the same design matrix except for the PPI regressors so that the signal changes associated with stimulus presentation and nuisance noises were excluded from the connectivity evaluation. The ROI-signal regressor in the design matrix was orthogonalized with respect to the interaction regressor to avoid a collinearity problem. This regressor multiplication approach of gPPI is known as accurate and more robust to noise than the deconvolution approach for a block-design experiment [44]. The gPPI analysis with the PCC ROI signal as the seed was performed for each task run independently. The mean *t*-value of the beta coefficient for the interaction term in the rTPJ ROI was used as an estimate of the task-related connectivity.

2.10 Other outcome measures

Other exploratory outcomes included the Montgomery-Åsberg Depression Rating Scale (MADRS) [45], Hamilton Anxiety Scale (HAMA) [46], Patient Health Questionnaire-9 (PHQ) [47], State-Trait Anxiety Inventory-Trait (STAI-T) [48], Metacognition Questionnaire-30 (MCQ) [49], Thought Control Questionnaire (TCQ) [50], Emotion Regulation Questionnaires (ERQ) [51], and Positive and Negative Affect Schedule - Expanded Form (PANAS) [52]. The PANAS was measured before

and after rtfMRI-nf within Visit1, and other measures were assessed before rtfMRI-nf as baseline and at one-week follow-up.

2.11 Criteria for reliable change of RNT

The reliable change index is a psychometric criterion used to evaluate whether a change over time of an individual score can be judged as reliably greater than a difference that could have occurred due to random measurement error alone (e.g., the mean difference between pre-intervention and post-intervention scores divided by the standard error of the measure is greater than 1.96)[53-55]. Following a clinical study using the RRS-B as an outcome measure [56], we calculated the standard error of the measure based on the SD of pre-intervention scores of the RRS-B (SD = 3.13) and coefficient α of RRS-B from published data (α = 0.77) [57]. Clinically significant change is achieved if a participant has met the criteria for reliable change and their scores shift from the clinical range at baseline to the nonclinical range at follow-up. Participants' scores were classified as having reliably deteriorated if they achieved reliable change in the opposite direction from hypothesized change. The estimated reliable change index of RRS-B was 4.15.

2.12 Whole-brain analysis: Brain regions responding to positive feedback and associated with a reduction in RNT

Considering the rtfMRI-nf training as a reinforcement learning process [58,59], the training effect may not be limited to the target brain activation. The nature of the feedback signal may not be transparent to the subjects since they cannot consciously perceive which action (i.e., brain activity) has been rewarded (e.g., a credit assignment problem in reinforcement learning [59,60]). Thus, possible learning mechanisms during rtfMRI-nf would be that; brain activations, not completely random but plausibly regulated by emotion regulation strategies (which subjects can perceive) during rtfMRI-nf, may be reinforced across rtfMRI-nf runs. Here, we used the strategy of defining the seed wherein responses to positive feedback change across rtfMRI-nf runs (i.e., learning effect not limited to the PCC-rTPJ connectivity), which may have contributed to a reduction in RNT.

We searched brain regions at the whole-brain voxel-wise level where learning effects (changed across rtfMRI-nf runs) were associated with a reduction in RNT. The series of beta-coefficients of the stimulus timing 'change to the positive feedback' of the GLM analysis with the same design matrix except for the PPI regressors (as in suppl. Methods 2.9) were used for the subsequent AFNI 3dLMEr analysis [61] for each run and each participant. The model included time (NF1, NF2, and NF3), group (active and sham), change in the RRS-B, three-way interaction (time-by-group-by-change in the RRS-B), age, sex, and average head motions as fixed effects, and a random effect of the subject on intercept. The significance criterion was set with voxel-wise $p < 0.001$ and cluster-size correction at $p < 0.05$ (AFNI 3dClustSim with the spatial autocorrelation function).

To further explore the effect of the three-way interaction term (time-by-group-by-change in the RRS-B), % BOLD signal changes from the identified cluster (retrosplenial cortex, RSC, in this sample) with a sphere of 6 mm radius around the peak coordinate were extracted (see suppl. Results 3.3). First, we investigated the longitudinal changes in the RSC activity

between the active and sham groups. Second, we investigated the association between the change in the RSC (at the last training: NF3 relative to the initial training: NF1) and the change in the RRS-B between groups.

The longitudinal change in the RSC activity was tested by the LME in R. The LME model included fixed effects of time (NF1, NF2, and NF3), group (active and sham), two-way interaction (time-by-group), age, sex, average head motions and a random effect of the subject on intercept.

The association between the change in the RSC activity and the change in the RRS-B between groups was tested with a robust regression analysis. The regression model included the change in the RRS-B at follow-up relative to baseline as dependent variables, and the change in the RSC activity at NF3 relative to NF1, group (active, sham) and two-way interaction (change in the RSC-by-group) as independent variables. Larger positive numbers for the change in the RSC indicated the increased activity in the RSC during the positive feedback presentations from NF1 to NF3, whereas larger negative numbers for the change in the RRS-B indicated greater improvement in RNT after rtfMRI-nf.

2.13 Whole-brain analysis: Functional connectivity reinforced through rtfMRI-nf and associated with a reduction in RNT

Next, we exploratorily investigated the effect of rtfMRI-nf on the connectivity between the RSC and our original rtfMRI-nf targets, i.e., rTPJ and PCC. We conducted gPPI analyses with the RSC as a seed, and calculated longitudinal change in the RSC-rTPJ connectivity and the RSC-PCC connectivity during rtfMRI-nf runs (NF1, NF2, and NF3) with a series of LME analyses.

The gPPI analysis from the RSC ROI signal was performed for the PCC ROI or rTPJ ROI for each rtfMRI-nf run (NF1, NF2, and NF3) independently. The design matrix of the GLM analysis for the gPPI analysis was similar to Methods 2.9, and we used the RSC as a seed. The *t*-value of the beta coefficient for the interaction term was used as an estimate of the task-related RSC-rTPJ connectivity or RSC-PCC connectivity.

The longitudinal change of the task-related connectivity between the RSC and rTPJ or RSC and PCC was tested by a series of LMEs in R. The LME model included fixed effects of time (NF1, NF2, and NF3), group (active and sham), two-way interaction (time-by-group), age, sex, average head motions and a random effect of the subject on intercept.

We also examined the association between the change in the connectivity (RSC-rTPJ or RSC-PCC) at NF3 from NF1 and the change in the RRS-B at follow-up from baseline between two groups with robust regression analyses. The regression models included the change in RRS-B at follow-up from baseline as dependent variables, and the change in the connectivity at NF3 from NF1, group (active, sham) and two-way interaction (change in connectivity-by-group) as independent variables. Larger negative numbers for the change in the connectivity indicated the reduced connectivity from NF1 to NF3, whereas larger negative numbers for the change in the RRS-B indicated a greater improvement in RNT after rtfMRI-nf.

3 Supplementary Results

3.1 Change in the primary neural outcome: LME analysis with age, sex, and average head motion as covariates

The main findings did not change even after controlling for covariates. There were no significant interactions or main effects on PPI estimates of the PCC-rTPJ connectivity (time-by-group interaction: F [3, 91] = 0.86, p = 0.47, time: F [3, 91] = 0.32, p = 0.81, group: F [1, 33] = 0.76, p = 0.39).

3.2 Change in the secondary clinical outcomes and other exploratory outcomes.

Secondary clinical outcomes. The LME analysis showed a trending time-by-group interaction and a significant time effect on the RRS-T (Fig. 3. B; time-by-group interaction: F [1, 37] = 3.31, p = 0.08, time: F [1, 37] = 20.64, p < 0.001, group: F [1, 35] = 0.02, p= 0.88). The post-hoc analysis within a group revealed that the active group showed a significantly reduced RRS-T score from baseline to follow-up (t [37] = 4.56, p_{FDR} < 0.001, effect size d = 0.67), and the sham group showed a marginally reduced score from baseline to follow-up (t [37] = 1.90, p_{FDR} = 0.07, effect size d = 0.26). A significant time effect on the RRS-D was observed (Fig. 3. B; time-by-group interaction: F [1, 37] = 2.32, p = 0.14, time: F [1, 37] = 16.36, p < 0.001, group: F [1, 35] = 0.05, p= 0.83). The post-hoc analysis within a group revealed that the active group showed a significantly reduced RRS-D score from baseline to follow-up (active: t [37] = 3.99, p_{FDR} < 0.001, effect size d = 0.56), and the sham group showed a marginally reduced score from baseline to follow-up (t [37] = 1.76, p_{FDR} = 0.09, effect size d = 0.26). There were no significant main effects on the RRS-R.

Other exploratory outcomes. Only a significant time effect was observed on the MADRS, HAMA, PHQ, STAI, MCQ Total score, MCQ Cognitive Self-Consciousness, MCQ Negative Beliefs about Uncontrollability and Danger, MCQ Need to Control Thoughts, TCQ Distraction, TCQ Punishment, ERQ Cognitive Reappraisal, PANAS Negative Affect, PANAS Positive Affect, PANAS Fear, PANAS Hostility, PANAS Guild, PANAS Sadness, PANAS Joviality, PANAS Self-Assurance, PANAS Shyness, and PANAS Surprise (see Table 2 for more details).

3.3 Brain regions responding to positive feedback and associated with improvement of RNT

A whole-brain analysis revealed a three-way interaction effect (time-by-group-by-change in the RRS-B) in the left retrosplenial cortex (RSC) (Fig. S4. B; MNI [-7, -53, 11], cluster size k = 79). This cluster also included the ventral area 23 (A23v) [25] in the PCC, and area 31 (A31) [25] in the precuneus, while the original PCC target (i.e., the PCC locus used for rtfMRI-nf) was located in the medial part of the precuneus (A7m/PEp) [25]. The spatial relationship between this RSC cluster extending onto the ventral part of the PCC and the original PCC target is illustrated in Fig. S5. No other main effects were found.

3.4 Longitudinal change in the RSC activity and its association with RNT

Longitudinal change in RSC activity. The longitudinal LME analyses between the two groups were summarized in Figs. S6. A and B. There were no significant time-by-group interactions, time, or group effect on % BOLD signal changes in the RSC (time-by-group interaction: F [2, 92] = 2.33, p = 0.10; time: F [2, 92] = 1.59, p = 0.21; group: F [1, 92] = 0.11, p = 0.74).

Association between change in the RSC and change in RNT. The robust regression analysis revealed that the interaction (change in the RSC-by-group) significantly predicted the change in the RRS-B (adjusted R^2 = 0.45, β =-21.60, *p* = 0.01; Table S6). This result indicates that the degree of association between the change in the RSC and the change in the RRS-B was significantly different between two groups. The simple slope analysis revealed that there was a trending negative association between the change in the RSC and the change in the RRS-B within the active group (adjusted R^2 = 0.29, β = -13.87, *p* = 0.07), while there was a positive association between the change in the RSC and the change in the RRS-B within the sham group (adjusted R^2 = 0.41, β = 7.90, *p* = 0.02) (Fig. S6. C). Altogether, greater activation in the RSC appeared to be associated with a reduced RRS-B in the active group, and less activation in the RSC was associated with a reduced RRS-B in the sham group.

3.5 Longitudinal change in the RSC-PCC connectivity and its association with RNT

Longitudinal change in the RSC-PCC connectivity. There were no significant main effects on time, group, or time-by-group interaction of the RSC-PCC connectivity (time-by-group interaction: *F* [2, 62] = 1.98, *p* = 0.15, group: *F* [1, 35] = 0.81, *p* = 0.37, time: *F* [2, 62] = 1.58, *p* = 0.21; Figs. S7. A and B).

Association between change in the RSC-PCC connectivity and change in RNT. There were no significant findings in the association between the change in the RSC-PCC connectivity and the change in RNT (Fig. S7. C and Table S8).

4 Supplementary Tables

Table S1. Consensus on the Reporting and Experimental Design of clinical and cognitive-behavioural Neurofeedback studies (CRED-nf) best practices checklist 2020* (an online tool to complete this checklist is available at rtfin.org/CREDnf).

Domain	Item #	Checklist item	Reported in page #
Pre-experiment			
	1a	Pre-register experimental protocol and planned analyses	4
	1b	Justify sample size	Supplementary methods 2.2.
Control groups			
	2a	Employ control group(s) or control condition(s)	4 and Supplementary introduction 1.3
	2b	When leveraging experimental designs where a double-blind is possible, use a double-blind	4
	2c	Blind those who rate the outcomes, and when possible, the statisticians involved	4 and Supplementary methods 2.1
	2d	Examine to what extent participants and experimenters remain blinded	4 and Supplementary methods 2.1
	2e	In clinical efficacy studies, employ a standard-of-care intervention group as a benchmark for improvement	Supplementary methods 2.11
Control measures			
	3a	Collect data on psychosocial factors	6
	3b	Report whether participants were provided with a strategy	6
	3c	Report the strategies participants used	Supplementary methods 2.6
	3d	Report methods used for online-data processing and artifact correction	Supplementary methods 2.4
	3e	Report condition and group effects for artifacts	Table 2
Feedback specifications			
	4a	Report how the online-feature extraction was defined	Supplementary methods 2.4
	4b	Report and justify the reinforcement schedule	Supplementary methods 2.5
	4c	Report the feedback modality and content	Supplementary methods 2.7
	4d	Collect and report all brain activity variable(s) and/or contrasts used for feedback, as displayed to experimental participants	7
	4e	Report the hardware and software used	Supplementary methods 2.4
Outcome measures			
Brain	5a	Report neurofeedback regulation success based on the feedback signal	7

	5b	Plot within-session and between-session regulation blocks of feedback variable(s), as well as pre-to-post resting baselines or contrasts	7
	5c	Statistically compare the experimental condition/group to the control condition(s)/group(s) (not only each group to baseline measures)	7
Behaviour	6a	Include measures of clinical or behavioural significance, defined a priori, and describe whether they were reached	8
	6b	Run correlational analyses between regulation success and behavioural outcomes	8
Data storage			
	7a	Upload all materials, analysis scripts, code, and raw data used for analyses, as well as final values, to an open access data repository, when feasible	Available upon requests

*Darker shaded boxes represent *Essential* checklist items; lightly shaded boxes represent *Encouraged* checklist items. We recommend using this checklist in conjunction with the standardized CRED-nf online tool (rtfin.org/CREDnf) and the CRED-nf article, which explains the motivation behind this checklist and provides details regarding many of the checklist items.

Table S2. Wordlist for the self-referential task. Participants selected 24 negative personality trait words that describe their personality from a 160-word list, which was taken from 555 sets of personality trait words [62]. In order to balance the valence, they were asked to select six words in each of four columns, which included 40 words in total (the average valences of each column were statistically the same).

1	imitative	41	angry	81	messy	121	bossy
2	melancholy	42	listless	82	misfit	122	unpleasing
3	mediocre	43	uninspiring	83	uninteresting	123	cowardly
4	obstinate	44	unintelligent	84	scornful	124	discourteous
5	unhealthy	45	domineering	85	antisocial	125	incompetent
6	headstrong	46	scolding	86	irritable	126	childish
7	nervous	47	depressed	87	stingy	127	superficial
8	nonconfident	48	unobliging	88	tactless	128	ungrateful
9	stubborn	49	pessimistic	89	careless	129	self-conceited
10	unimaginative	50	unattentive	90	foolish	130	hard-hearted
11	down-hearted	51	suspicious	91	troublesome	131	unfair
12	unobservant	52	inattentive	92	ungracious	132	irresponsible
13	inconsistent	53	overconfident	93	negligent	133	prejudiced
14	unpunctual	54	smug	94	wishy-washy	134	bragging
15	unindustrious	55	unsociable	95	gloomy	135	jealous
16	disturbed	56	unproductive	96	helpless	136	unpleasant
17	superstitious	57	wasteful	97	disagreeable	137	unreliable
18	frustrated	58	fickle	98	touchy	138	impolite
19	illogical	59	neglectful	99	irrational	139	crude
20	rash	60	short-tempered	100	tiresome	140	nosey
21	unenthusiastic	61	hot-headed	101	disobedient	141	humorless
22	inaccurate	62	unsocial	102	complaining	142	quarrelsome
23	unagreeable	63	envious	103	lifeless	143	distrustful
24	jumpy	64	overcritical	104	vain	144	intolerant
25	possessive	65	scheming	105	lazy	145	unforgiving
26	purposeless	66	sly	106	maladjusted	146	boring
27	moody	67	weak	107	aimless	147	unreasonable
28	unenterprising	68	foolhardy	108	boastful	148	self-centered
29	unintellectual	69	immature	109	dull	149	snobbish
30	unwise	70	dominating	110	gossipy	150	unkindly
31	oversensitive	71	showy	111	unappealing	151	ill-mannered
32	inefficient	72	sloppy	112	hypochondriac	152	ill-tempered
33	reckless	73	unsympathetic	113	irritating	153	unfriendly
34	pompous	74	uncompromising	114	petty	154	hostile
35	uncongenial	75	hot-tempered	115	shallow	155	dislikable
36	untidy	76	neurotic	116	deceptive	156	offensive
37	unaccommodating	77	finicky	117	grouchy	157	underhanded
38	noisy	78	resentful	118	egotistical	158	annoying
39	squeamish	79	unruly	119	meddlesome	159	disrespectful
40	cynical	80	fault-finding	120	cold	160	selfish

Table S3. The result of the Post-Neurofeedback Session Questionnaires.

		Active (n=20)		Sham (n=19)		Statistics	*p*
		Active %(n)	Sham %(n)	Active %(n)	Sham %(n)		
1.	Was it 'Active' or 'Sham'?	60% (12)	40% (8)	42% (8)	58% (11)	$\chi^2(1)=0.64$	0.43
		Mean (SD)		Mean (SD)			
2.	How much are you confident with your response?	5.25 (1.92)		4.89 (2.21)		*t*(37)=0.54	0.59
3.	How pleasant was the current neurofeedback session for you?	6.00 (2.51)		6.16 (2.54)		*t*(37)=-0.19	0.85
4.	How unpleasant was the current neurofeedback session for you?	2.65 (2.50)		2.63 (2.34)		*t*(37)=0.02	0.98
5.	How challenging was the current neurofeedback session for you?	5.95 (2.31)		5.53 (1.84)		*t*(37)=0.63	0.53
6.	How successful do you feel you were in stopping ruminating during this scan?	5.45 (1.82)		6.32 (1.70)		*t*(37)=-1.53	0.13
7.	How often did you find yourself dwelling on negative aspects of yourself?	5.05 (2.33)		4.89 (1.97)		*t*(37)=0.22	0.82
8.	How successful do you feel you were in modulating your brain activity during this session?	5.25 (2.12)		6.00 (1.33)		*t*(37)=-1.31	0.20
9.	How helpful do you feel like this neurofeedback session was in preventing yourself from ruminating?	5.35 (1.95)		5.37 (2.43)		*t*(37)=-0.03	0.98
10.	How helpful do you feel like this neurofeedback session will be to know how to stop your rumination in your daily life?	6.15 (2.08)		5.89 (2.11)		*t*(37)=0.38	0.71
11.	How did you feel about the amount of time you had in the scanner to try and modulate your brain activity?	5.90 (1.17)		5.53 (1.90)		*t*(37)=0.75	0.46

Items 2 to 11 were rated from 0=not at all (or much too short) to 10=extremely (or much too long).

Examples of emotion regulation strategies used during rtfMRI-nf	Group	Category
Seeing the negative traits as 'not bad'. Everyone is like this to a degree, or viewing them as an opportunity for growth.	Active	Reappraisal
Thinking of positive songs and happy memories.	Active	Positive thoughts
Counted back, e.g., 321.	Active	Distraction
Positive affirmations, arguing how the negative trait can actually be helpful in my life.	Sham	Reappraisal
Thinking about happy events in my life.	Sham	Positive thoughts
Singing songs in my head.	Sham	Distraction

Table S4. Numbers of emotion regulation strategies used during rtfMRI-nf.

	Active (n=20)	Sham (n=19)
Reappraisal	15	9
Positive thoughts or memories	6	8
Distraction	3	5

Emotion regulation strategies used during rtfMRI-nf (from the Post-Neurofeedback Session Questionnaires) were categorized by two independent raters (licensed clinical psychologists). If a person used multiple strategies, it was categorized multiple times (e.g., 'reappraisal' and 'positive thoughts or memories'). An inter-rater agreement measured by Krippendorff's α was 0.78[63]. Numbers of strategies did not differ between the groups (Fisher's exact test, $p = 0.38$).

Table S5. A robust regression analysis predicting chage in RRS-B from change in PCC-rTPJ connectivity.

	Primary clinical outcome Change in RRS-B			
	MM-Estimate	SE	*t*	*p*
Interaction analysis				
Intercept	-0.48	0.73	-0.66	0.51
Change in PCC-rTPJ connectivity	0.18	0.60	0.30	0.77
Group	-2.62	1.01	-2.60	**0.01**
Change in PCC-rTPJ connectivity : Group	-0.17	0.83	-0.21	0.83
Simple slope analysis (Active)				
Intercept	-3.11	0.78	-3.98	0.00
Change in PCC-rTPJ connectivity	-0.003	0.64	-0.004	1.00
Simple slope analysis (Sham)				
Intercept	-0.49	0.62	-0.79	0.44
Change in PCC-rTPJ connectivity	0.19	0.51	0.37	0.72

Change in PCC-rTPJ connectivity : change in connectivity between precuneus/porterior cingulate cortex (PCC) and right temproparietal junction (rTPJ) during rtfMRI-nf from baseline; RRS: Ruminative Response Scale (RRS); Change in RRS-B: chage in brooding subscale of RRS at one-week follow-up from baseline.

Table S6. A robust regression analysis predicting chage in RRS-B from change in RSC activity.

	Primary clinical outcome Change in RRS-B			
	MM-Estimate	SE	*t*	*p*
Interaction analysis				
Intercept	0.18	0.71	0.26	0.80
Change in RSC activity	7.49	3.92	1.91	0.07
Group	-1.93	1.12	-1.72	0.10
Change in RSC activity : Group	-21.60	7.20	-3.00	**0.01**
Simple slope analysis (Active)				
Intercept	-1.94	1.01	-1.93	0.08
Change in RSC activity	-13.87	7.03	-1.97	0.07
Simple slope analysis (Sham)				
Intercept	0.38	0.57	0.67	0.51
Change in RSC activity	7.90	3.12	2.53	**0.02**

Change in RSC activity: % BOLD signal changes in the retrosplenial cortex (RSC) during NF3 from NF1; RRS: Ruminative Response Scale (RRS); Change in RRS-B: chage in brooding subscale of RRS at one-week follow-up from baseline.

Table S7. A robust regression analysis predicting chage in RRS-B from change in RSC-rTPJ connectivity.

	Primary clinical outcome Change in RRS-B			
	MM-Estimate	SE	*t*	*p*
Interaction analysis				
Intercept	-0.19	0.71	-0.27	0.79
Change in RSC-rTPJ connectivity	-0.44	0.46	-0.94	0.36
Group	-2.19	1.07	-2.06	0.05
Change in RSC-rTPJ connectivity : Group	1.58	0.64	2.46	**0.02**
Simple slope analysis (Active)				
Intercept	-2.41	0.87	-2.75	**0.02**
Change in RSC-rTPJ connectivity	1.14	0.49	2.32	**0.04**
Simple slope analysis (Sham)				
Intercept	-0.18	0.65	-0.29	0.78
Change in RSC-rTPJ connectivity	-0.44	0.42	-1.05	0.31

Change in RSC-rTPJ connectivity: change in connectivity between retrosplenial cortex (RSC) and right temporoparietal junction (rTPJ) at NF3 (PPI estimates) from NF1; RRS: Ruminative Response Scale (RRS); Change in RRS-B: chage in brooding subscale of RRS at one-week follow-up from baseline.

Table S8. A robust regression analysis predicting chage in RRS-B from change in RSC-PCC connectivity.

	Primary clinical outcome Change in RRS-B			
	MM-Estimate	SE	*t*	*p*
Interaction analysis				
Intercept	-0.41	0.81	-0.50	0.62
Change in RSC-PCC connectivity	-0.02	0.81	-0.02	0.98
Group	-2.92	1.21	-2.43	**0.02**
Change in RSC-PCC connectivity : Group	-0.64	1.06	-0.60	0.55
Simple slope analysis (Active)				
Intercept	-3.35	1.04	-3.21	**0.01**
Change in RSC-PCC connectivity	-0.66	0.81	-0.81	0.43
Simple slope analysis (Sham)				
Intercept	-0.42	0.69	-0.60	0.56
Change in RSC-PCC connectivity	-0.01	0.69	-0.01	0.99

Change in RSC-PCC connectivity: Change in connectivity between retrosplenial cortex (RSC) and precuneus/posterior cingulate cortex (PCC) at NF3 (PPI estimates) from NF1; RRS: Ruminative Response Scale (RRS); Change in RRS-B: chage in brooding subscale of RRS at one-week follow-up from baseline.

5 Supplementary Figures

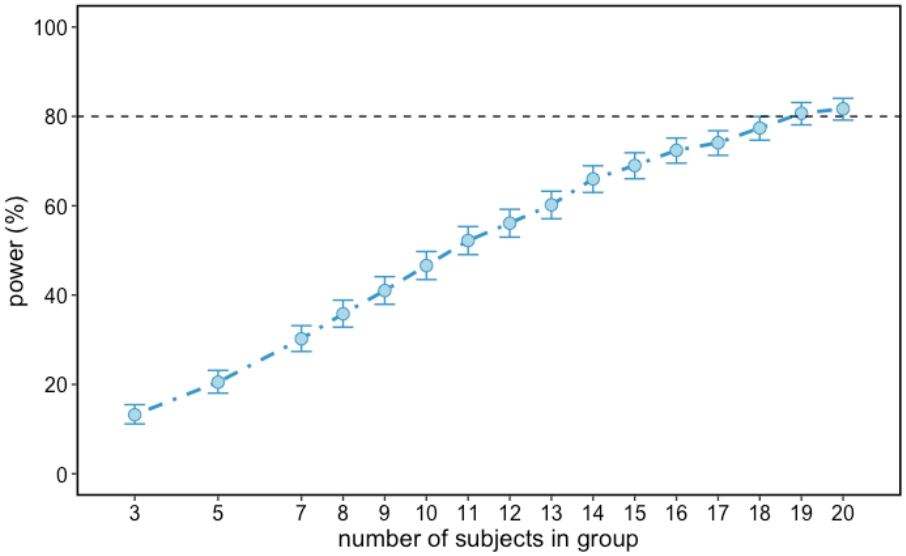

Figure S1. A result of the power curve analysis.

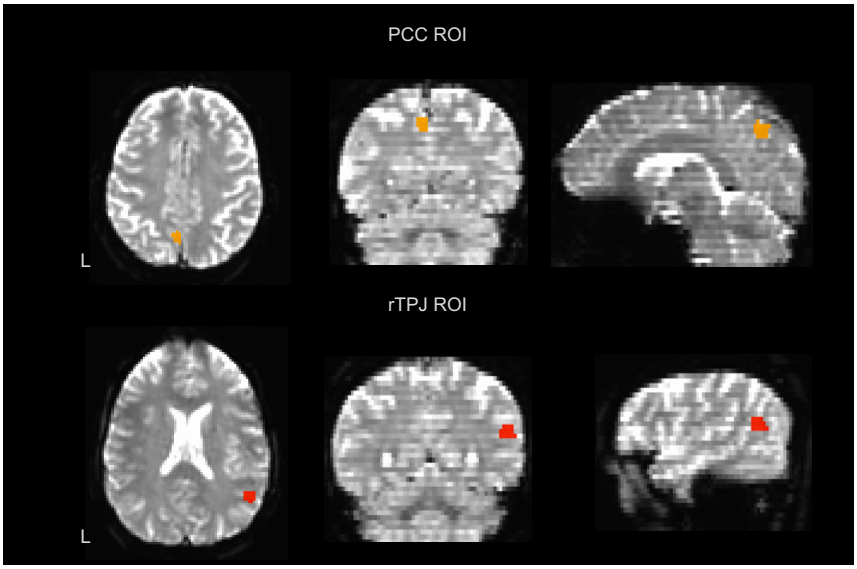

Figure S2. An example of ROIs to calculate real-time fMRI neurofeedback signals in a T2*-weighted image.

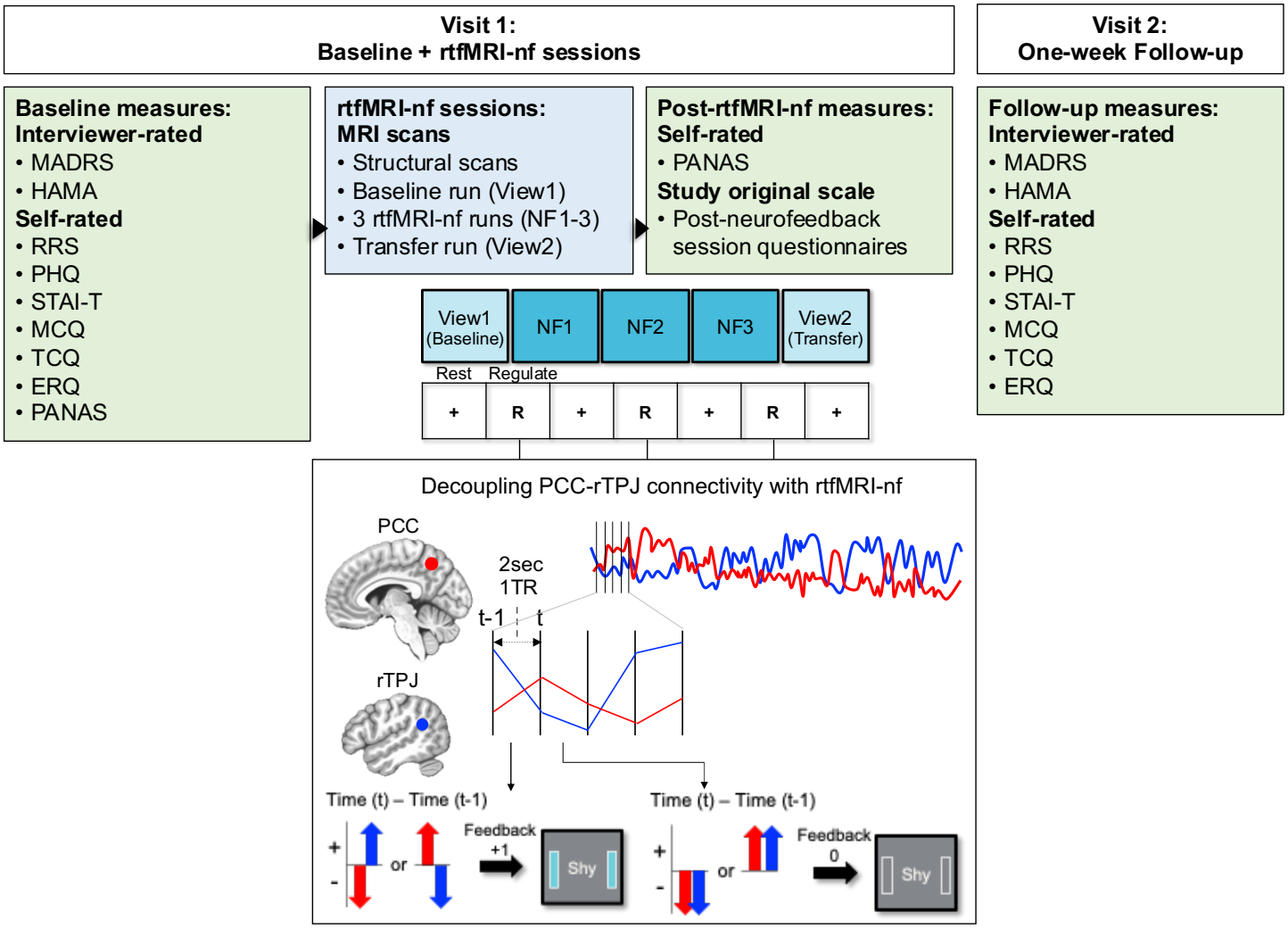

Figure S3. Outline of the study protocol.

A rtfMRI-nf session included five experimental runs: View1, rtfMRI-nf run 1 to 3 (NF1, NF2, and NF3), and View2. Each experimental run started with a first 'Rest' block (90-sec), followed by 'Regulation' block (100-sec) during the presentation of four negative trait words (25-sec for each word) and 'Rest' block (30-sec) alternatively. In the rtfMRI-nf scans (NF1, NF2, and NF3), participants were instructed to apply emotion regulation strategies, such as cognitive reappraisal, while viewing negative trait words, and were instructed to regulate their brain activity represented by the sidebars during the 'Regulation' block. In the initial view scan (View1: Baseline), participants were instructed to regulate repetitive negative thinking (RNT) in the face of negative trait words during the 'Regulation' block, and in the last view scan (View2: Transfer), participants were instructed to use the emotion regulation strategy that worked best throughout the three rtfMRI-nf runs (NF1, NF2, and NF3) to regulate RNT during the 'Regulation' block. A Red circle, red arrows, and red lines indicate the precuneus/posterior singulate cortex (PCC) ROI and BOLD activities, and a blue circle, blue arrows, and blue lines indicate the right temporoparietal junction (rTPJ) ROI and BOLD activities. The sidebars on the screen were updated every 2-sec with positive feedback (+1: light blue color) or no feedback (0: blank color). Abbreviations. MADRS: Montgomery- Åsberg Depression Rating Scale, HAMA: Hamilton Anxiety Scale, RRS: Ruminative Response Scale, PHQ: Patient Health Questionnaire-9, STAI-T: State-Trait Anxiety Inventory-Trait, MCQ: Metacognition Questionnaire-30, TCQ: Thought Control Questionnaire. ERQ: Emotion Regulation Questionnaires, PANAS: Positive and Negative Affect Schedule - Expanded Form.

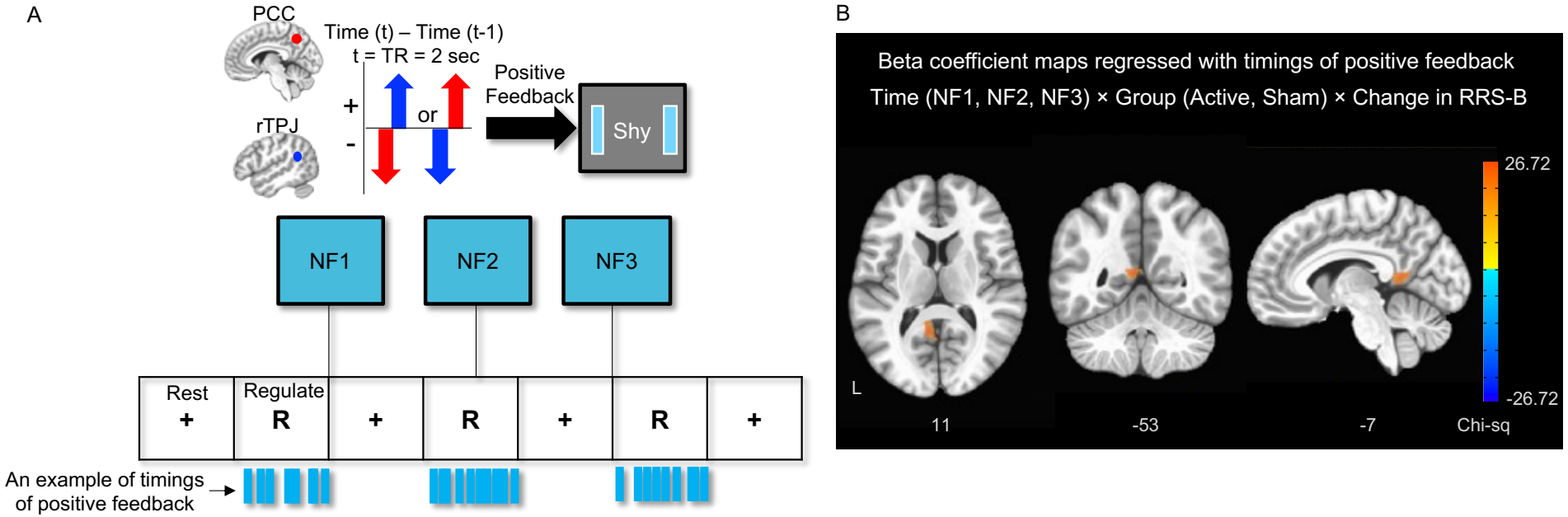

Figure S4. A. An example of positive feedback and its timing. When BOLD signals from PCC and rTPJ change in a different direction from (t) – (t-1), t as repetition time (TR) = 2 seconds, subjects see blue side bars (positive feedback). When BOLD signals from the PCC and rTPJ change in the same direction from (t) – (t-1), blue side bars dessapear and subjects see blank sidebars (absence of positive feedback). Feedback information was updated every 2 seconds. **B. A brain region responding to positive feedback across real-time fMRI neurofeedback (rtfMRI-nf) runs and also associated with change in repetitive negative thinking (RNT).** A whole-brain analysis of beta coefficient maps regressed with timings of positive feedback revealed that the left retrosplenial cortex (RSC) showed a significantly different association with the change in the brooding subscale of the Ruminative Response Scale (RRS-B) across rtfMRI-nf runs between the active and sham groups.

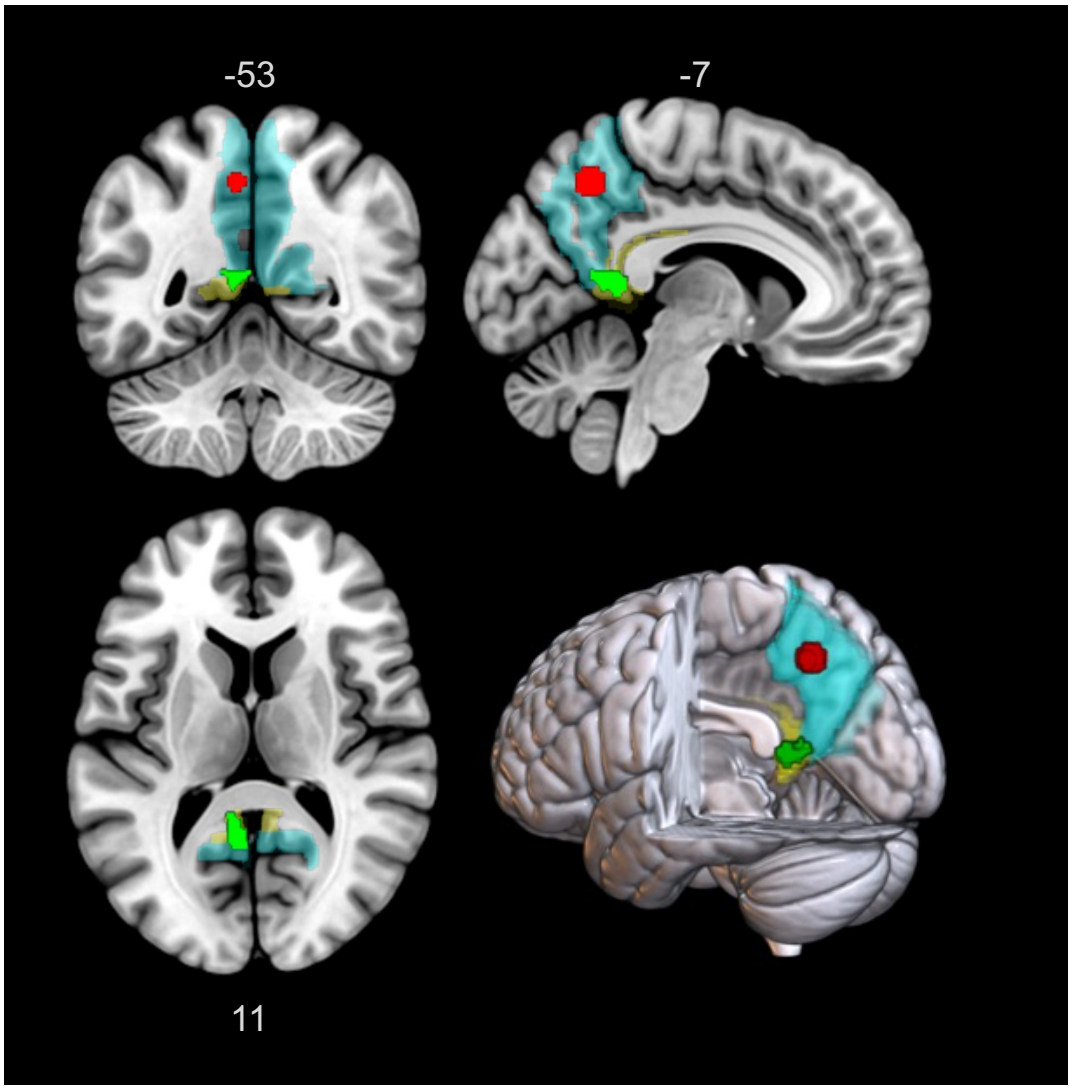

Figure S5. The locus of retrosplenial cortex (RSC) identified through an exploratory whole-brain analysis and the locus of precuneus/posterior cingulate cortex (PCC) used for real-time fMRI neurofeedback (rtfMRI-nf). A red sphere (original PCC target) is the region-of-interest (ROI) where the BOLD signal was extracted and used for a feedback signal calculation (i.e., PCC-right temporoparietal junction [rTPJ] connectivity). A green area (RSC) reflects the clusters showing a significantly different association with the change in the brooding subscale of the Ruminative Response Scale (RRS-B) across rtfMRI-nf runs between two groups. A shaded area with light blue indicates anatomically defined precuneus area (brainnetome atlas, PCun_4_1, 4_2, 4_3, and 4_4), and a shaded area with yellow indicates anatomically defined ventral area of the PCC (brainntome atlas, A23v) [64].

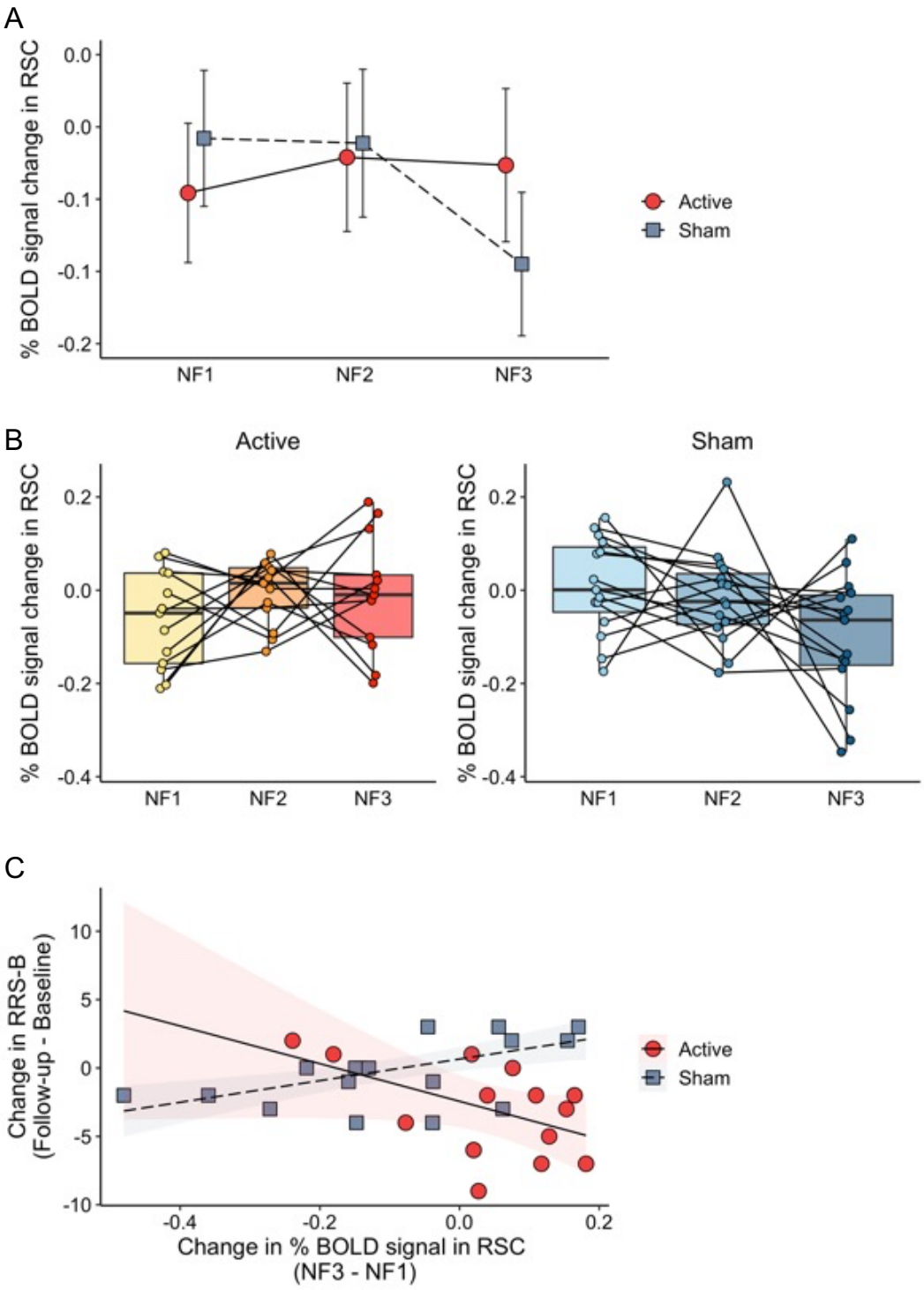

Figure S6. Longitudinal change in the retrosplenial cortex (RSC) activity, and an association between the change in the RSC and the change in repetitive negative thinking (RNT). A. Longitudinal change in % BOLD signal changes of the RSC between two groups through the rtfMRI-nf runs. NF1, NF2, and NF3: neurofeedback run with a self-referential task. **B. Boxplots and individual plots of % BOLD signal changes of the RSC.** Left: active group, Right: sham group. **C. An association between the change in % BOLD signal changes in the RSC (NF3 from NF1) and the change in the RRS-B (follow-up from baseline).**

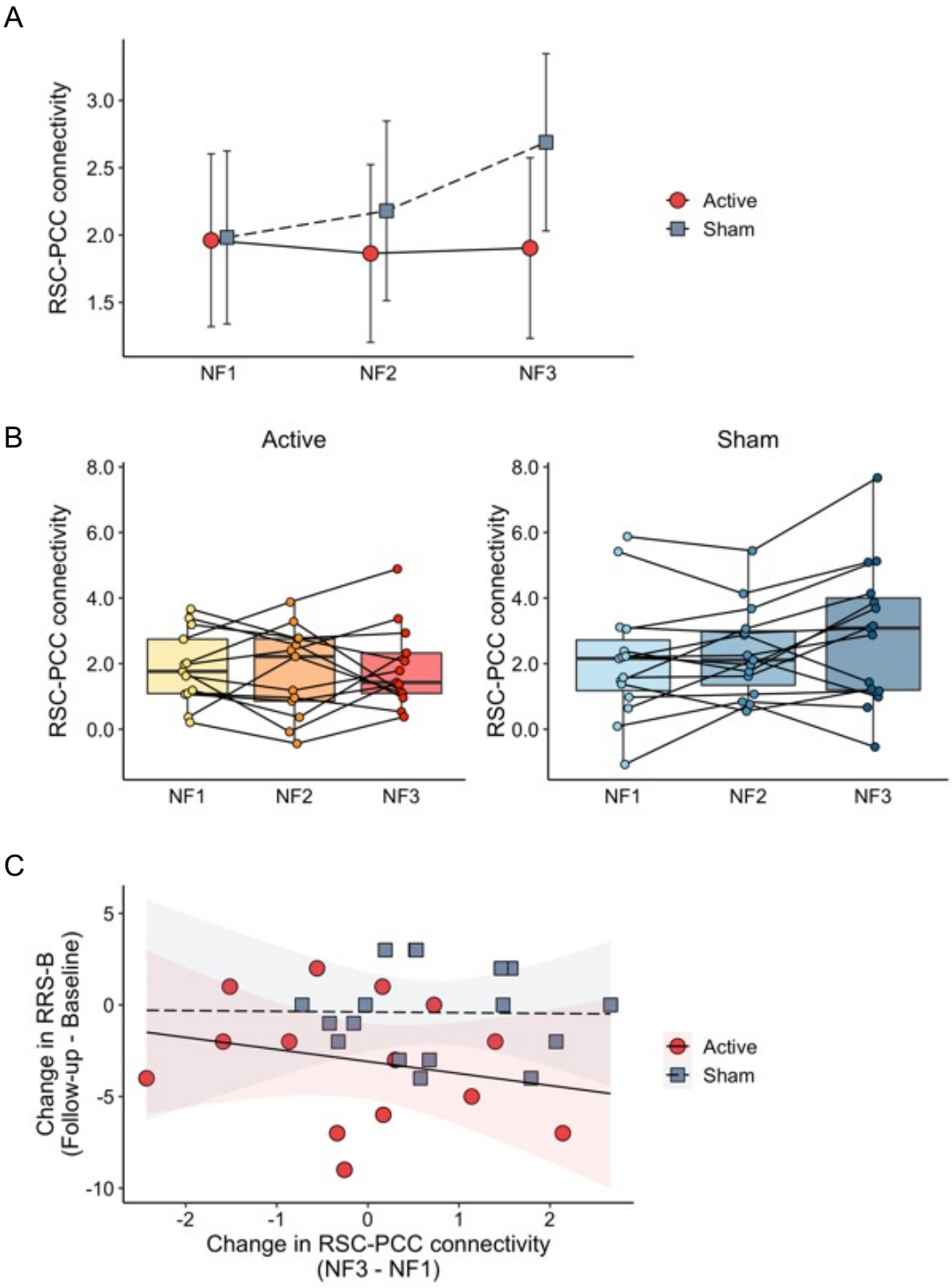

Figure S7. Longitudinal change in the functional connectivity between retrosplenial cortex (RSC) and posterior cingulate cortex (PCC), and an association between the change in the RSC-PCC connectivity and the change in the brooding subscale of the Ruminative Response Scale (RRS-B). A. Longitudinal change in the RSC-PCC connectivity (PPI estimates) between two groups through the rtfMRI-nf runs. NF1, NF2 and NF3: neurofeedback run with a self-referential task. **B. Boxplots and individual plots of the RSC-PCC connectivity.** Left: active group, Right: sham group. **C. An association between the change in the RSC-PCC connectivity at NF3 from NF1 and the change in the RRS-B at follow-up from baseline.** The error bars represent the 95% confidence interval of the mean values. The shaded areas represent the 95% confidence interval of regression slopes.

6 References

1 Zotev V, Krueger F, Phillips R, Alvarez RP, Simmons WK, Bellgowan P, et al. Self-regulation of amygdala activation using real-time FMRI neurofeedback. PLoS One. 2011;6(9):e24522.

2 Scheinost D, Stoica T, Saksa J, Papademetris X, Constable RT, Pittenger C, et al. Orbitofrontal cortex neurofeedback produces lasting changes in contamination anxiety and resting-state connectivity. Transl Psychiatry. 2013;3:e250.

3 Young KD, Siegle GJ, Bodurka J, Drevets WC. Amygdala Activity During Autobiographical Memory Recall in Depressed and Vulnerable Individuals: Association With Symptom Severity and Autobiographical Overgenerality. Am J Psychiatry. 2016;173(1):78-89.

4 Bauer CCC, Okano K, Ghosh SS, Lee YJ, Melero H, Angeles CL, et al. Real-time fMRI neurofeedback reduces auditory hallucinations and modulates resting state connectivity of involved brain regions: Part 2: Default mode network -preliminary evidence. Psychiatry Res. 2020;284:112770.

5 Morgenroth E, Saviola F, Gilleen J, Allen B, Luhrs M, M WE, et al. Using connectivity-based real-time fMRI neurofeedback to modulate attentional and resting state networks in people with high trait anxiety. Neuroimage Clin. 2020;25:102191.

6 Zhao Z, Yao S, Li K, Sindermann C, Zhou F, Zhao W, et al. Real-Time Functional Connectivity-Informed Neurofeedback of Amygdala-Frontal Pathways Reduces Anxiety. Psychother Psychosom. 2019;88(1):5-15.

7 Berman MG, Peltier S, Nee DE, Kross E, Deldin PJ, Jonides J. Depression, rumination and the default network. Soc Cogn Affect Neurosci. 2011;6(5):548-55.

8 Hamilton JP, Farmer M, Fogelman P, Gotlib IH. Depressive Rumination, the Default-Mode Network, and the Dark Matter of Clinical Neuroscience. Biol Psychiatry. 2015;78(4):224-30.

9 Jacob Y, Morris LS, Huang KH, Schneider M, Rutter S, Verma G, et al. Neural correlates of rumination in major depressive disorder: A brain network analysis. Neuroimage Clin. 2020;25:102142.

10 Jacobs RH, Jenkins LM, Gabriel LB, Barba A, Ryan KA, Weisenbach SL, et al. Increased coupling of intrinsic networks in remitted depressed youth predicts rumination and cognitive control. PLoS One. 2014;9(8):e104366.

11 Rosenbaum D, Haipt A, Fuhr K, Haeussinger FB, Metzger FG, Nuerk HC, et al. Aberrant functional connectivity in depression as an index of state and trait rumination. Sci Rep. 2017;7(1):2174.

12 Zhou HX, Chen X, Shen YQ, Li L, Chen NX, Zhu ZC, et al. Rumination and the default mode network: Meta-analysis of brain imaging studies and implications for depression. Neuroimage. 2020;206:116287.

13 Zhu X, Zhu Q, Shen H, Liao W, Yuan F. Rumination and Default Mode Network Subsystems Connectivity in First-episode, Drug-Naive Young Patients with Major Depressive Disorder. Sci Rep. 2017;7:43105.

14 Misaki M, Tsuchiyagaito A, Al Zoubi O, Paulus M, Bodurka J, Tulsa 1000 I. Connectome-wide search for functional connectivity locus associated with pathological rumination as a target for real-time fMRI neurofeedback intervention. Neuroimage Clin. 2020;26:102244.

15 Andrews-Hanna JR, Reidler JS, Sepulcre J, Poulin R, Buckner RL. Functional-anatomic fractionation of the brain's default network. Neuron. 2010;65(4):550-62.

16 Davey CG, Pujol J, Harrison BJ. Mapping the self in the brain's default mode network. Neuroimage. 2016;132:390-97.

17 Cole MW, Schneider W. The cognitive control network: Integrated cortical regions with dissociable functions. Neuroimage. 2007;37(1):343-60.

18 Li R, Utevsky AV, Huettel SA, Braams BR, Peters S, Crone EA, et al. Developmental Maturation of the Precuneus as a Functional Core of the Default Mode Network. J Cogn Neurosci. 2019;31(10):1506-19.

19 Utevsky AV, Smith DV, Huettel SA. Precuneus is a functional core of the default-mode network. J Neurosci. 2014;34(3):932-40.
20 Saxe R. The right temporo-parietal junction: a specific brain region for thinking about thoughts. In: Leslie A, German T, editors. Handbook of theory of mind. Taylor & Francis Group; 2010. p. 1-35.
21 Saxe R, Kanwisher N. People thinking about thinking people. The role of the temporo-parietal junction in "theory of mind". Neuroimage. 2003;19(4):1835-42.
22 Young L, Camprodon JA, Hauser M, Pascual-Leone A, Saxe R. Disruption of the right temporoparietal junction with transcranial magnetic stimulation reduces the role of beliefs in moral judgments. Proc Natl Acad Sci U S A. 2010;107(15):6753-8.
23 Tsuchiyagaito A, Misaki M, Zoubi OA, Tulsa I, Paulus M, Bodurka J. Prevent breaking bad: A proof of concept study of rebalancing the brain's rumination circuit with real-time fMRI functional connectivity neurofeedback. Hum Brain Mapp. 2021;42(4):922-40.
24 Jaeckle T, Williams SCR, Barker GJ, Basilio R, Carr E, Goldsmith K, et al. Self-blame in major depression: a randomised pilot trial comparing fMRI neurofeedback with self-guided psychological strategies. Psychological medicine. 2021:1-11.
25 Mehler DMA, Sokunbi MO, Habes I, Barawi K, Subramanian L, Range M, et al. Targeting the affective brain-a randomized controlled trial of real-time fMRI neurofeedback in patients with depression. Neuropsychopharmacology. 2018;43(13):2578-85.
26 Young KD, Siegle GJ, Zotev V, Phillips R, Misaki M, Yuan H, et al. Randomized Clinical Trial of Real-Time fMRI Amygdala Neurofeedback for Major Depressive Disorder: Effects on Symptoms and Autobiographical Memory Recall. Am J Psychiatry. 2017;174(8):748-55.
27 Thibault RT, Lifshitz M, Birbaumer N, Raz A. Neurofeedback, Self-Regulation, and Brain Imaging: Clinical Science and Fad in the Service of Mental Disorders. Psychother Psychosom. 2015;84(4):193-207.
28 Green P, Macleod CJSIMR. SIMR: An R package for power analysis of generalized linear mixed models by simulation. . Methods Ecol Evol 2016;7:493–98.
29 Field A. Discovering statistics using IBM SPSS statistics (4th ed.). SAGE Publications Inc: CA, USA; 2013.
30 Misaki M, Barzigar N, Zotev V, Phillips R, Cheng S, Bodurka J. Real-time fMRI processing with physiological noise correction - Comparison with off-line analysis. J Neurosci Methods. 2015;256:117-21.
31 Misaki M, Bodurka J. The impact of real-time fMRI denoising on online evaluation of brain activity and functional connectivity. J Neural Eng. 2021;18(4):046092.
32 Misaki M, Bodurka J, Paulus M. A Library for fMRI Real-Time Processing Systems in Python (RTPSpy) With Comprehensive Online Noise Reduction, Fast and Accurate Anatomical Image Processing, and Online Processing Simulation. Front Neurosci. 2022;16:834827.
33 Glover GH, Li TQ, Ress D. Image-based method for retrospective correction of physiological motion effects in fMRI: RETROICOR. Magn Reson Med. 2000;44(1):162-7.
34 Avants BB, Epstein CL, Grossman M, Gee JC. Symmetric diffeomorphic image registration with cross-correlation: evaluating automated labeling of elderly and neurodegenerative brain. Med Image Anal. 2008;12(1):26-41.
35 Sheline YI, Barch DM, Price JL, Rundle MM, Vaishnavi SN, Snyder AZ, et al. The default mode network and self-referential processes in depression. Proc Natl Acad Sci U S A. 2009;106(6):1942-7.
36 Zilverstand A, Parvaz MA, Goldstein RZ. Neuroimaging cognitive reappraisal in clinical populations to define neural targets for enhancing emotion regulation. A systematic review. Neuroimage. 2017;151:105-16.
37 Gembris D, Taylor JG, Schor S, Frings W, Suter D, Posse S. Functional magnetic resonance imaging in real time (FIRE): sliding-window correlation analysis and reference-vector optimization. Magn Reson Med. 2000;43(2):259-68.

38 Ramot M, Kimmich S, Gonzalez-Castillo J, Roopchansingh V, Popal H, White E, et al. Direct modulation of aberrant brain network connectivity through real-time NeuroFeedback. Elife. 2017;6:e28974.
39 Cox RW. AFNI: what a long strange trip it's been. Neuroimage. 2012;62(2):743-7.
40 Birn RM, Smith MA, Jones TB, Bandettini PA. The respiration response function: the temporal dynamics of fMRI signal fluctuations related to changes in respiration. Neuroimage. 2008;40(2):644-54.
41 Power JD, Schlaggar BL, Petersen SE. Recent progress and outstanding issues in motion correction in resting state fMRI. Neuroimage. 2015;105:536-51.
42 McLaren DG, Ries ML, Xu G, Johnson SC. A generalized form of context-dependent psychophysiological interactions (gPPI): a comparison to standard approaches. Neuroimage. 2012;61(4):1277-86.
43 Jo HJ, Saad ZS, Simmons WK, Milbury LA, Cox RW. Mapping sources of correlation in resting state FMRI, with artifact detection and removal. Neuroimage. 2010;52(2):571-82.
44 Di X, Biswal BB. Psychophysiological Interactions in a Visual Checkerboard Task: Reproducibility, Reliability, and the Effects of Deconvolution. Front Neurosci. 2017;11:573.
45 Montgomery SA, Asberg M. A new depression scale designed to be sensitive to change. Br J Psychiatry. 1979;134:382-9.
46 Maier W, Buller R, Philipp M, Heuser I. The Hamilton Anxiety Scale: reliability, validity and sensitivity to change in anxiety and depressive disorders. J Affect Disord. 1988;14(1):61-8.
47 Kroenke K, Spitzer RL, Williams JB. The PHQ-9: validity of a brief depression severity measure. J Gen Intern Med. 2001;16(9):606-13.
48 Spielberger CD, Gorssuch RL, Lushene PR, Vagg PR, Jacobs GA. Manual for the State-Trait Anxiety Inventory. Consulting Psychologists Press, Inc.; 1983.
49 Wells A, Cartwright-Hatton S. A short form of the metacognitions questionnaire: properties of the MCQ-30. Behav Res Ther. 2004;42(4):385-96.
50 Reynolds M, Wells A. The Thought Control Questionnaire--psychometric properties in a clinical sample, and relationships with PTSD and depression. Psychol Med. 1999;29(5):1089-99.
51 Gross JJ, John OP. Individual differences in two emotion regulation processes: implications for affect, relationships, and well-being. J Pers Soc Psychol. 2003;85(2):348-62.
52 Watson D, Clark LA. The PANAS-X: Manual for the Positive and Negative Affect Schedule - Expanded Form. The University of Iowa; 1994.
53 Evans C, Margison F, Barkham M. The contribution of reliable and clinically significant change methods to evidence-based mental health. Evidence-Based Mental Health. 1998;1(13):70-72.
54 Guhn M, Forer B, Zumbo BD. Reliable Change Index. In: Michalos AC, editor Encyclopedia of Quality of Life and Well-Being Research. Dordrecht: Springer; 2014.
55 Jacobson NS, Truax P. Clinical significance: a statistical approach to defining meaningful change in psychotherapy research. J Consult Clin Psychol. 1991;59(1):12-9.
56 Thorslund J, McEvoy PM, Anderson RA. Group metacognitive therapy for adolescents with anxiety and depressive disorders: A pilot study. J Clin Psychol. 2020;76(4):625-45.
57 Treynor W, Gonzalez R, Nolen-Hoeksema S. Rumination Reconsidered: A Psychometric Analysis. Cognit Ther Res. 2003;27:247–59.
58 Kvamme TL, Ros T, Overgaard M. Can neurofeedback provide evidence of direct brain-behavior causality? Neuroimage. 2022;258:119400.
59 Lubianiker N, Paret C, Dayan P, Hendler T. Neurofeedback through the lens of reinforcement learning. Trends Neurosci. 2022;45(8):579-93.
60 Minsky M. Steps Toward Artificial Intelligence. Proc IRE. 1961;1:8-30.
61 Chen G, Saad ZS, Britton JC, Pine DS, Cox RW. Linear mixed-effects modeling approach to FMRI group analysis. Neuroimage. 2013;73:176-90.
62 Anderson NH. Likableness ratings of 555 personality-trait words. J Pers Soc Psychol. 1968;9(3):272-9.

63 Hays AF, Krippendorff K. Answering the Call for a Standard Reliability Measure for Coding Data. Communication Methods and Measures 2007;1(1):77-89.
64 Fan L, Li H, Zhuo J, Zhang Y, Wang J, Chen L, et al. The Human Brainnetome Atlas: A New Brain Atlas Based on Connectional Architecture. Cereb Cortex. 2016;26(8):3508-26.